A dC/dV Measurement for Quantum-Dot Light-Emitting Diodes

Jingrui Ma(马精瑞)[1,2], Haodong Tang(唐浩东)[1,2], Xiangwei Qu(瞿祥炜)[1,2], Guohong Xiang(项国洪)[1,2], Siqi Jia(贾思琪)[1,2], Pai Liu(刘湃)[1,2], Kai Wang(王恺)[1,2,3], and Xiao Wei Sun(孙小卫)[1,2,3*]

[1]*Key Laboratory of Energy Conversion and Storage Technologies (SUSTech) of Ministry of Education, Guangdong-Hong Kong-Macao Joint Laboratory for Photonic-Thermal-Electrical Energy Materials and Devices, SUSTech-Huawei Joint Lab for Photonics Industry, and Department of Electrical and Electronic Engineering, Southern University of Science and Technology, Shenzhen 518055, China*
[2]*Institute of Nanoscience and Applications, Southern University of Science and Technology, Shenzhen 518055, China*
[3]*Shenzhen Planck Innovation Technologies Co. Ltd., Shenzhen 518173, China*

(Received 21 September 2022; accepted manuscript online 4 November 2022)

We present dC/dV analysis based on the capacitance-voltage (C–V) measurement of quantum-dot light-emitting diodes (QLEDs), and find that some key device operating parameters (electrical and optical turn-on voltage, peak capacitance, maximum efficiency) can be directly related to the turning points and maximum/minimum of the dC/dV (versus voltage) curve. By the dC/dV study, the behaviors such as low turn-on voltage, simultaneous electrical and optical turn-on process, and carrier accumulation during the device aging can be well explained. Moreover, we perform the C–V and dC/dV measurement of aged devices, and confirm that our dC/dV analysis is correct for them. Thus, our dC/dV analysis method can be applied universally for QLED devices. It provides an in-depth understanding of carrier dynamics in QLEDs through simple C–V measurement.

DOI: 10.1088/0256-307X/39/12/128401

Unique optoelectronic properties such as tunable wavelength, narrow emission full-width at half maximum (FWHM), low driving voltage, and high luminance make colloidal quantum-dot light-emitting diodes (QLEDs) a competitive candidate for next-generation display technology.[1–4] The performance of QLEDs is advancing quickly because of considerable advancements in quality of quantum-dots (QDs) materials and device architectures.[5–8] In recent years, there are numerous studies on QLEDs with an aim for commercialization,[9,10] for example, the development of mass-compatible fabrication processes (ink-jet printing, photolithography, electrophoretic deposition, etc.),[11–14] the enhancement of device operation lifetime (especially blue devices),[6,10] the establishment of standard performance evaluation methods,[15,16] the understanding of failure mechanisms,[17] the improvement of encapsulation methods,[18] and shelf stability.[19] Currently, conventional QLEDs have hybrid device structures, which comprise organic hole transport layers (HTLs) and an inorganic nanocrystal electron transport layer (ETL).[20] These layer-stacked structures are similar to the organic light-emitting diodes (OLEDs).[21–24] Therefore, methods and models in OLEDs like C–V could be utilized to characterize the carrier dynamics in QLEDs. For example, Chen *et al.*[17] have reported the degradation mechanisms of QLEDs based on C–V characterizations. They showed that the aging of red QLEDs is primarily caused by the degradation of HTLs. However, in the blue, the degradation of QD/ETL junction is more responsible. Similarly, Chen *et al.*[18] have used C–V characterization to discuss the hole leakage behavior and its effect on recombination during the aging of devices. Moreover, Qian *et al.*[25] have verified the formation of traps during the aging of QLEDs using this method. Our group has also studied the charge transfer and neutralization processed in QLEDs using C–V characterization methods.[26] All of these reports demonstrate that C–V characterization is a powerful method to analyze the carrier injection, transport, accumulation, and recombination behavior in QLEDs.[27–29] However, because of the significant difference between organic and inorganic materials, it is less appropriate to describe carrier behavior entirely with the OLED approach.[30,31] In particular, the carrier behaviors in QLEDs, such as confinement-enhanced coulomb effects, carrier accumulation and recombination during the device aging, are hard to be adequately characterized by standard OLED theory.[32–34] Therefore, it is essential to find a way to analyze the carrier dynamics for QLEDs aiming at a deeper understanding of the working mechanism of QLEDs.

The dC/dV measurement has been used to analyze the doping profile or interface trap distribution in the traditional diodes and metal-oxide-semiconductor structures.[35,36] In the diode case, it is reversely biased, so that the dopants or traps in depletion region could respond to the voltage applied. In QLEDs, the carrier transport is by hopping and the C–V results are usually obtained under the forward bias to analyze the charge transport and recombination behavior.[23] In this work, we develop a dC/dV method based on the general C–V measurement to analyze the carrier behavior in the QLEDs. The results show that the voltage of specific turning points at the dC/dV curve corresponds to the critical voltage points for device turn-on, peak capacitance, and maximum efficiency. The amplitude of dC/dV also reflects the carrier accumu-

*Corresponding author. Email: xwsun@sustech.edu.cn
© 2022 Chinese Physical Society and IOP Publishing Ltd

lation and recombination rate (efficiency). This dC/dV method is further applied to analyze the degradation process during the device aging. The results show that the dC/dV method works well to analyze and understand the carrier picture in QLEDs.

We used red Cd-based QLEDs with a conventional structure of ITO/PEDOT:PSS/TFB/QDs/ZnO/Ag in our study. After the fabrication, basic measurements including current density–voltage–luminance–EQE (J–V–L–EQE), low-frequency C–V sweep and time-resolved electroluminescence (TREL) based on time-correlated single-photon counting (TCSPC), operational aging test, luminance uniformity check, etc. are performed to evaluate the performance of the devices. Detailed experimental information is provided in the Supplementary Material.

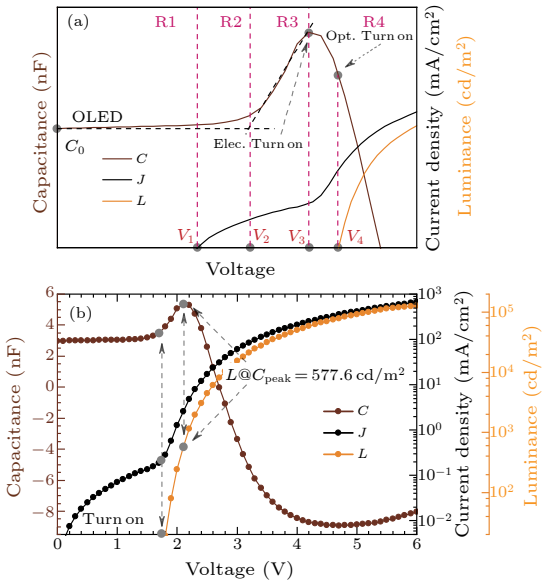

Fig. 1. Different C–V behaviors between OLED and QLED. (a) Illustrative ideal OLED J–V–L–C curve without any scales. (b) J–V–L–C characteristics of QLED (C–V sweep at $f = 1$ kHz, $V_{ac} = 100$ mV) obtained in our experiment. R1: Neutral, R2: Dark current, R3: Majority carrier injection, R4: Dual carrier injection & recombination.

Figure 1(a) shows the ideal OLED J–V–L–C curve under forward bias condition.[27,28,37] Four regions including neutral region (R1), dark current region (R2), majority carrier injection region (R3), dual-carrier injection and recombination region (R4) can be divided according to the dominating charge behavior in the region.[28,37] In R1, the capacitance keeps almost constant (often called the geometric capacitance, C_0). The charge in R2 (as seen by the slight capacitance rise) is mainly contributed by the small amount of charge trapped in the defects and interface before V_2. After V_2, the majority (or fast) carriers, usual holes in OLED, are injected so the capacitance is increasing rapidly. In R3, the majority carriers are accumulated in the majority carrier transport layer (HTL or HTL/EML interface for OLEDs). The voltage of peak capacitance (or slightly smaller than this voltage point) usually corresponds to the electrical turn-on voltage located in R3. This is because the minority carriers (electrons in OLEDs) are injected at this voltage. Then the electron-hole recombination process starts.[27] In R4, the recombination begins dominating the C–V behavior and the device reaches the optical turn-on voltage (defined when luminance reaches 1 cd/m^2, bigger than V_3). Such a picture is widely used to understand the carrier's injection, transport, accumulation, and recombination process in the OLEDs.[27,29,37–40] In this picture, the majority carriers are injected at V_2 and the minority carriers are injected at V_3. This injected voltage difference will cause a gap between electrical turn-on voltage (in R3) and optical turn-on voltage (in R4) in OLEDs even in the devices with high performance.[41]

We measured C–V behavior of our QLEDs, as shown in Fig. 1(b). In fact, similar C–V has been shown by other researchers with no exception.[17,25,26] Similar to OLEDs, there is also unbalanced charge injection in QLEDs.[15,28] The strong negative capacitance at lower frequency reflects the efficient radiative recombination of the device.[42] To our surprise, the electrical and optical turn-on voltages are at almost the same point and prior to the voltage where the capacitance reaches the maximum value. In addition, a sub-threshold electrical and optical turn-on voltage was obtained in our experiment, which is smaller than the photon energy/e (e is the electron charge), consistent with previous reports on QLEDs.[6,40] At the voltage where C_{peak} is observed, the luminance of the device is 577.6 cd/m^2, which indicates relatively efficient minority carrier injection and radiative recombination under this voltage.

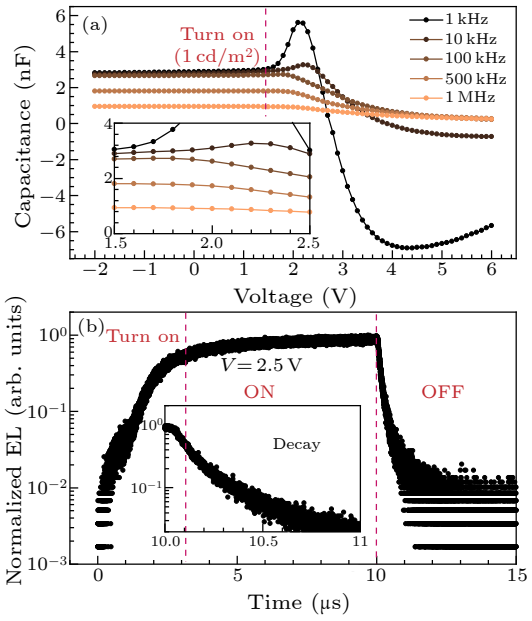

Fig. 2. (a) Frequency-dependent C–V characteristics of QLED (inset: the capacitance around the turn-on voltage, $V_{ac} = 100$ mV). (b) TREL result of the QLED under 2.5 V voltage pulse (inset: the decayed part of the device). The voltage ON time is 10 μs.

This phenomenon differs greatly from OLEDs. Since the minority carriers in OLEDs are only injected after reaching peak capacitance (C_{peak}), i.e., recombination happens after the peak capacitance point.[27] As is well known, the testing frequency f is the key parameter determining the C–V response.[28,37] Figure 2(a) shows the frequency-dependent C–V results on QLEDs with the

fixed $V_{ac} = 100\,\text{mV}$ (small signal). The absence of C_{peak} at high frequency indicates little/no charge accumulation in the device. At higher frequency, the carrier is too slow to respond to the signal and the carrier accumulation is suppressed. It is worth mentioning again there is a distinct difference compared to OLEDs. In QLEDs as in our case, the voltage at C_{peak} is always higher than the turn-on voltage (below 10 kHz). We can also see that the capacitance becomes smaller with the increase in frequency, and the voltage to reach C_{peak} increases with the frequency as well. This is because the transient carrier behavior for injection, transport, recombination, accumulation, trapping, and detrapping is limited by the carrier mobility, trap energy and trap density in the device.[27] At a higher frequency, the charge may be too slow to respond to the test signal, so the capacitance is smaller and needs a higher voltage to reach its maximum.[17] In order to determine the proper test frequency, the TREL test was performed to analyze the transient behavior of the device (2.5 V square pulsed bias with the 10 µs ON-time), as shown in Fig. 2(b). It can be seen that it takes about 3 µs for the device to turn-on and 5 µs to turn-off. Thus, the C–V tests should use a frequency lower than 100 kHz (the total response time estimated as 10 µs). Considering Fig. 1(a), we used 1 kHz in this work for the tests analyzed in the following.

The C–V behavior reflects the charge accumulation and recombination in the devices. Higher capacitance represents more accumulated and less consumed (recombination) charges in the device, and vice versa. Meanwhile, the EQE represents the efficiency of emitted photon versus injected electron, which reflects the recombination behavior of the carriers in the devices. Higher EQE represents a faster radiative recombination rate of carriers in the devices. Thus, in a high performance device such as ours in this work, the recombination rate of carriers could be described as the speed of charge consumption, and could be reflected by the first derivative of capacitance versus voltage (dC/dV). It is worth mentioning that the charge accumulation and consumption rates are the same for a steady-state QLED. However, this balance is of dynamics, i.e., depending on the applied voltage and its fluctuations, one could be larger than the other. The dC/dV here reflects this dynamics, or the tendency of charge variation in the device. The sign of dC/dV indicates the tendency of either charge accumulation (> 0) or consumption (< 0).

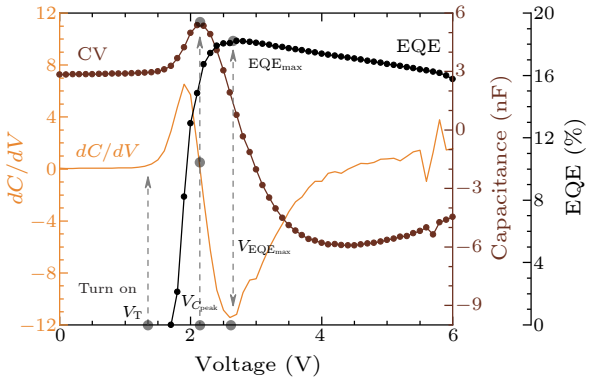

Fig. 3. The low-frequency dC/dV, C–V, and EQE results of the typical QLED ($f = 1\,\text{kHz}$, $V_{ac} = 100\,\text{mV}$).

Figure 3 shows the low-frequency dC/dV, C–V, and EQE results of the fabricated device. As discussed above, the dC/dV represents the rate of charge accumulation (positive) or consumption (negative). The electrical turn-on voltage of dC/dV at ∼1.5 V indicates that the charge injection and accumulation have started (rate > 0). Also, the light emission under this voltage is confirmed using an imaging photometer. A uniform emission of the device at 1.5 V was observed (Fig. S1 in the Supplementary Material). This is direct evidence of radiative recombination in the QLEDs, which confirms that the electrical and optical turn-on voltage is at the same voltage. It is worth mentioning that this electrical and optical turn-on voltage V_T (1.5 V) is smaller than the general definition of turn-on voltage (the voltage when luminance reaches $1\,\text{cd/m}^2$). Previous reports have also detected weak light emission even below 1.2 V.[43] This behavior can be explained as the injected majority (or fast) carriers (electrons in QLEDs) attracting the minority (or slow) carriers (holes), and then emitting a photon due to confinement-enhanced coulomb effects in QDs.[32] With this picture, the coincidence of electrical and optical turn-on voltages can be understood. At V_T, the injection and recombination of carriers are both observed.

Since the dC/dV result represents the accumulation or consumption rate of carriers. The dC/dV curve after V_T could be regarded as the competition between the injection and recombination as we discuss its change in voltage sequence in the following.

1. When dC/dV is above zero, the injection of carriers dominates the capacitance of the device. The recombination of carriers is weaker and the capacitance tends to increase at this range.
2. At the point where dC/dV is equal to zero (V at C_{peak} in Fig. 3), the injection and recombination of carriers reach a balanced situation. At this voltage, the capacitance reaches the peak value.
3. After the peak capacitance, dC/dV is lower than zero, representing that the recombination of carriers starts to dominate. The accumulation of carriers still exists, but its rate is slower than the recombination rate.
4. At the voltage where dC/dV reaches the minimum value (V at EQE$_{max}$ in Fig. 3), the recombination rate of carriers reaches its peak value. The carriers are rapidly consumed and the capacitance of the devices decreases quickly. At this point, the EQE of the device also reaches its peak value.
5. After V at EQE$_{max}$, the recombination rate of carriers saturates or even starts to decrease (by Auger effect for example). However, the rate of injection is less affected, leading to the decrease of EQE.

With understanding of the dC/dV curve, we designed a group of experiments to analyze the C–V variation for degraded QLEDs. The fabricated devices are well packaged and aged at constant current stress of $100\,\text{mA/cm}^2$. J–V–L–EQE and C–V tests were both performed daily to record the performance of the devices at different stages of degradation. It is worth mentioning that the daily J–V–L and C–V tests have little effect on the aging behavior, as we verified with control devices.

Figure 4 shows the aging time-dependent EQE–V, C–V, and dC/dV results. The 6-day curve is missing in Fig. 4 as the device failed (short) at day-6 as shown in L–t–V (Fig. S2) and J–V–L (Fig. S4). It is clearly seen that the dC/dV minimum corresponds to the maximum EQE point for all the aged devices. The dC/dV minimum could be a gauging point for QLEDs study. Using the dC/dV model we developed, we can analyze the QLEDs degradation in the following.

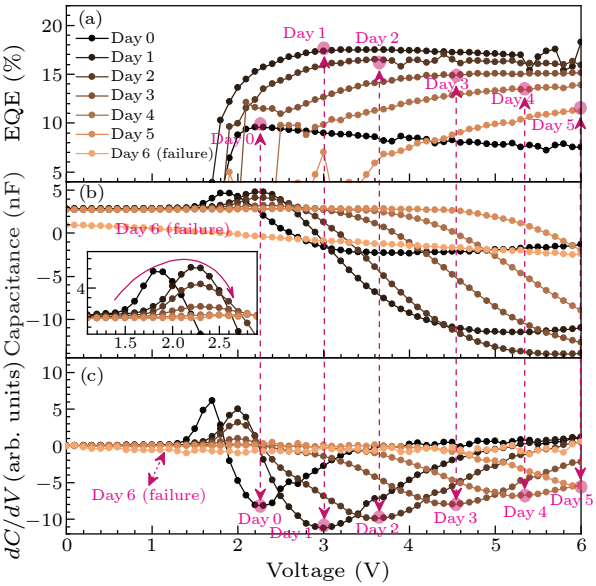

Fig. 4. Aging time-dependent characteristics of QLED. The device is stressed with a constant current density of 100 mA/cm^2. (a) EQE–V, (b) C–V (inset is the close-up image of charge accumulation region), and (c) dC/dV–V curves.

Firstly, the device benefits a positive aging process for 1 day. This unique behavior of QLEDs is related with the passivation of traps and the resistance switch effect of ETL (ZnO-based nanocrystals).[17,44,45] The voltage required to reach $\mathrm{EQE_{max}}$ is higher and the value of $\mathrm{EQE_{max}}$ is almost doubled, compared with the fresh device [Fig. 4(a)]. Moreover, the increase of both peak capacitance and voltage required to reach the peak capacitance indicates that there is more charge accumulation in the device [Fig. 4(b)]. The variation of C_{peak} reflects the change of charge accumulation in the device. For day-1 device, the carrier injection is more efficient (more charge accumulation), while for day-2 to day-5 devices, the injection is degraded (less charge accumulation) as seen in Fig. 4(c). This charge accumulation is also reflected on the dC/dV curve. The more negative minimum of dC/dV value for day-1 device compared with fresh (day-0) device represents more efficient charge recombination [Fig. 4(c)]. The "positive" current aging process enhances not only the charge accumulation (injection), but also the rate of charge consumption (recombination) in the device. After the positive current aging process, from day-1 to day-5, the $\mathrm{EQE_{max}}$ of the devices shifts towards lower values and at higher voltages, as shown in Fig. 4(a). The minimum of dC/dV [Fig. 4(c)] is also increasing at the same time, which represents a reduced charge recombination rate, and correspondingly a decreasing $\mathrm{EQE_{max}}$. The decrease of peak capacitance [inset of Fig. 4(b)] accompanied by a smaller voltage shift of the maximum of dC/dV reflects less charge accumulation in the device for day-1 to day-5 devices. This may be caused by the degradation of HTL,[17] which leads to suppression of both charge accumulation (peak capacitance) and charge injection (dC/dV). These coincident behaviors between dC/dV and EQE–V further verify the classic asymmetric carrier picture in QLEDs.

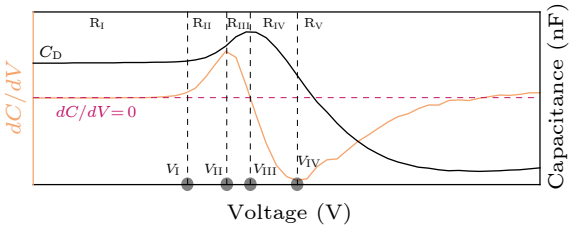

Fig. 5. Typical QLED dC/dV–V–C curve. Five regions (R_{I}-R_{V}) represent the different charge injection and recombination status under different biases. Critical nodes are marked as $V_{\mathrm{I}} - V_{\mathrm{IV}}$. $\mathrm{R_I}$: Dark current region, $\mathrm{R_{II}}$: Injection & weak recombination region, $\mathrm{R_{III}}$: Injection & recombination region, $\mathrm{R_{IV}}$: Strong recombination region, $\mathrm{R_V}$: Recombination & accumulation region.

Based on the discussion, we can separate the dC/dV characteristics of QLEDs into five different regions in Fig. 5. The five regions are separated according to the turning points on the dC/dV curve and verified carrier dynamics in QLEDs, which represents the rate competition between charge accumulation and consumption. R_{I} is the dark current region and a little charge is injected into the device ($dC/dV \approx 0$), the current is mainly from intrinsic carriers and CD corresponds to depletion capacitance. In R_{II}, both electrons and holes are injected into QDs followed by recombination. The electrical and optical turn-on voltage is the same, which is around V_{I} due to the confinement-enhanced coulomb effects.[32] The charge accumulation (capacitance increases, $dC/dV \gg 0$) is caused by the different injection rates of electrons and holes. Usually, the majority (fast) carriers, electrons, will be accumulated in the devices. At V_{II} coinciding with the dC/dV maximum, the charge accumulation rate starts to decrease. This is caused by the shrinking of the rate gap between electron injection and hole injection due to Coulomb interaction. More electrons will attract more holes' injection and hinder electrons until maximum capacitance (V_{III}, $dC/dV = 0$). In R_{IV}, the charge accumulation rate changes to a negative value, indicating that the charges recombine more than what they accumulate in the device, i.e., the charge recombination is dominating the carrier behavior ($dC/dV < 0$). Meanwhile, the EQE value will increase rapidly after V_{III} and reaches the maximum value at V_{IV}, where the dC/dV reaches the minimum value at this point. In region R_{V}, the carrier recombination almost saturates. The consumption rate of charge is decreased and the amplitude of dC/dV is also decreased.

In conclusion, we have studied the low-frequency C–V characteristics of QLEDs, and found that dC/dV can serve as a gauging method for evaluation of carrier injection and recombination in devices. Critical voltage points such as V_{T} (both optical and electrical), C_{peak}, and $\mathrm{EQE_{max}}$

have a close relationship to the dC/dV curve's zero point and minimum point. The rate of charge accumulation and consumption can also be well reflected by the amplitude of dC/dV. By this dC/dV method, the degradation behavior of the carrier in the device is well analyzed and understood. With the aid of the dC/dV study, we have clarified the physical picture of carrier injection, transport, accumulation, and recombination in QLEDs. The reported physical processes in QLEDs like sub-threshold turn-on,[46] "linked" behavior of electrons and holes,[32] and charge accumulation during the device degradation[25] are also verified and well understood in dC/dV analyses.

Acknowledgements. This work was supported by the Key-Area Research and Development Program of Guangdong Province (Grant Nos. 2019B010925001 and 2019B010924001), the Shenzhen Peacock Team Project (Grant Nos. KQTD20160301 and 11203005), and Shenzhen Key Laboratory for Advanced Quantum Dot Displays and Lighting (Grant Nos. ZDSYS201707 and 281632549).

References

[1] Coe S, Woo W K, Bawendi M G, and Bulović V 2002 *Nature* **420** 800
[2] Kagan C R, Lifshitz E, Sargent E H, and Talapin D V 2016 *Science* **353** aac5523
[3] Shirasaki Y, Supran G J, Bawendi M G, and Bulović V 2013 *Nat. Photon.* **7** 13
[4] de Arquer F P G, Talapin D V, Klimov V I, Arakawa Y, Bayer M, and Sargent E H 2021 *Science* **373** eaaz8541
[5] Song J J, Wang O Y, Shen H B, Lin Q L, Li Z H, Wang L, Zhang X T, and Li L S 2019 *Adv. Funct. Mater.* **29** 1808377
[6] Deng Y Z, Peng F, Lu Y, Zhu X T, Jin W X, Qiu J, Dong J W, Hao Y L, Di D W, Gao Y, Sun T, Zhang M, Liu F, Wang L, Ying L, Huang F, and Jin Y 2022 *Nat. Photon.* **16** 505
[7] Liu D Q, Cao S, Wang S Y, Wang H Q, Dai W, Zou B S, Zhao J L, and Wang Y J 2020 *J. Phys. Chem. Lett.* **11** 3111
[8] Wu L, Liu W, Lu Z, Yan Y, Zhang J, Xu W, Yang Y, and Yan X 2020 *SID Symp. Dig. Tech. Papers* **51** 1071
[9] Yang J, Choi M K, Yang U J, Kim S Y, Kim Y S, Kim J H, Kim D H, and Hyeon T 2021 *Nano Lett.* **21** 26
[10] Davidson-Hall T and Aziz H 2020 *Appl. Phys. Lett.* **116** 010502
[11] Jia S Q, Tang H D, Ma J R, Ding S H, Qu X W, Xu B, Wu Z H, Li G Y, Liu P, Wang K, and Sun X W 2021 *Adv. Opt. Mater.* **9** 2101069
[12] Zhao J, Chen L, Li D, Shi Z, Liu P, Yao Z, Yang H, Zou T, Zhao B, Zhang X, Zhou H, Yang Y, Cao W, Yan X, Zhang S, and Sun X W 2021 *Nat. Commun.* **12** 4603
[13] Hahm D, Lim J, Kim H, Shin J W, Hwang S, Rhee S, Chang J H, Yang J, Lim C H, Jo H, Choi B, Cho N S, Park Y S, Lee D C, Hwang E, Chung S, Kang C M, Kang M S, and Bae W K 2022 *Nat. Nanotechnol.* **17** 952
[14] Fan J and Qian L 2022 *Nat. Nanotechnol.* **17** 906
[15] Jin W, Deng Y, Guo B, Lian Y, Zhao B, Di D, Sun X W, Wang K, Chen S, Yang Y, Cao W, Chen S, Ji W, Yang X, Gao Y, Wang S, Shen H, Zhao J, Qian L, Li F, and Jin Y 2022 *npj Flex. Electron.* **6** 35
[16] Anaya M, Rand B P, Holmes R J, Credgington D, Bolink H J, Friend R H, Wang J, Greenham N C, and Stranks S D 2019 *Nat. Photon.* **13** 818
[17] Chen S, Cao W, Liu T, Tsang S W, Yang Y, Yan X, and Qian L 2019 *Nat. Commun.* **10** 765
[18] Chen Z, Su Q, Qin Z, and Chen S 2021 *Nano Res.* **14** 320
[19] Chen D, Chen D, Dai X, Zhang Z, Lin J, Deng Y, Hao Y, Zhang C, Zhu H, Gao F, and Jin Y 2020 *Adv. Mater.* **32** 2006178
[20] Chen M, Chen X, Ma W, Sun X, Wu L, Lin X, Yang Y, Li R, Shen D, Chen Y, and Chen S 2022 *ACS Nano* **16** 9631
[21] Mandoc M M, de Boer B, Paasch G, and Blom P W M 2007 *Phys. Rev. B* **75** 193202
[22] Lan X, Chen M, Hudson M H, Kamysbayev V, Wang Y, Guyot-Sionnest P, and Talapin D V 2020 *Nat. Mater.* **19** 323
[23] Guyot-Sionnest P 2012 *J. Phys. Chem. Lett.* **3** 1169
[24] Meulenkamp E A 1999 *J. Phys. Chem. B* **103** 7831
[25] Cao W, Xiang C, Yang Y, Chen Q, Chen L, Yan X, and Qian L 2018 *Nat. Commun.* **9** 2608
[26] Wu Z, Liu P, Qu X, Ma J, Liu W, Xu B, Wang K, and Sun X W 2021 *Adv. Opt. Mater.* **9** 2100389
[27] Xiao X, Ye T, Sun J, Qu X, Ren Z, Wu D, Ding S, Sun X W, Choy W C H, and Wang K 2022 *Appl. Phys. Lett.* **120** 243501
[28] Zhang X W, Xu J W, Xu H R, Wang H, Xie C L, Wei B, Jiang X Y, and Zhang Z L 2013 *J. Phys. D* **46** 055102
[29] Kim D, Kwon O, Kim M, and Lee H 2022 *Org. Electron.* **108** 106593
[30] Dai X L, Zhang Z X, Jin Y Z, Niu Y, Cao H J, Liang X Y, Chen L W, Wang J P, and Peng X G 2014 *Nature* **515** 96
[31] Zhang Z X, Ye Y X, Pu C D, Deng Y Z, Dai X L, Chen X P, Chen D, Zheng X R, Gao Y, Fang W, Peng X G, and Jin Y Z 2018 *Adv. Mater.* **30** 1801387
[32] Deng Y, Lin X, Fang W, Di D, Wang L, Friend R H, Peng X, and Jin Y 2020 *Nat. Commun.* **11** 2309
[33] Pu C, Dai X, Shu Y, Zhu M, Deng Y, Jin Y, and Peng X 2020 *Nat. Commun.* **11** 937
[34] Jung S M, Lee T H, Bang S Y, Han S D, Shin D W, Lee S, Choi H W, Suh Y H, Fan X B, Jo J W, Zhan S, Yang J, Samarakoon C, Kim Y, Occhipinti L G, Amaratunga G, and Kim J M 2021 *npj Comput. Mater.* **7** 122
[35] Ambrózy A 1970 *Solid-State Electron.* **13** 347
[36] Chim W K, Wong K M, Yeow Y T, Hong Y D, Lei Y, Teo L W, and Choi W K 2003 *IEEE Electron Device Lett.* **24** 667
[37] Shrotriya V and Yang Y 2005 *J. Appl. Phys.* **97** 054504
[38] Campbell I H, Smith D L, and Ferraris J P 1995 *Appl. Phys. Lett.* **66** 3030
[39] You C, Titov A, Kim B H, and Orazem M E 2020 *J. Solid State Electrochem.* **24** 3083
[40] Brütting W, Berleb S, and Mückl A G 2001 *Org. Electron.* **2** 1
[41] Guo Q G, Dai Y F, Sun Q, Qiao X F, Chen J S, Zhu T F, and Ma D G 2018 *Adv. Electron. Mater.* **4** 1800177
[42] Feng L F, Wang J, Zhu C Y, Cong H X, Chen Y, and Wang C D 2005 *Optoelectron. Lett.* **1** 124
[43] Lian Y, Lan D, Xing S, Guo B, Ren Z, Lai R, Zou C, Zhao B, Friend R H, and Di D 2022 *Nat. Commun.* **13** 3845
[44] Rhee S, Chang J H, Hahm D, Kim K, Jeong B G, Lee H J, Lim J, Char K, Lee C, and Bae W K 2019 *ACS Appl. Mater. Interfaces* **11** 40252
[45] Su Q, Sun Y Z, Zhang H, and Chen S M 2018 *Adv. Sci.* **5** 1800549
[46] Luo H X, Zhang W J, Li M L, Yang Y X, Guo M X, Tsang S W, and Chen S 2019 *ACS Nano* **13** 8229

Supplementary Material:
A dC/dV measurement for quantum dot light-emitting diodes

Jingrui Ma,[1,2] Haodong Tang, [1,2] Xiangwei Qu,[1,2] Guohong Xiang,[1,2] Siqi Jia,[1,2] Pai Liu,[1,2] Kai Wang,[1,2,3] and Xiao Wei Sun[1,2,3a)]

[1)] Key Laboratory of Energy Conversion and Storage Technologies (SUSTech) of Ministry of Education, Guangdong-Hong Kong-Macao Joint Laboratory for Photonic-Thermal-Electrical Energy Materials and Devices, SUSTech-Huawei Joint Lab for Photonics Industry, and Department of Electrical and Electronic Engineering, Southern University of Science and Technology, Shenzhen 518055, China
[2)] Institute of Nanoscience and Applications, Southern University of Science and Technology, Shenzhen 518055, China
[3)] Shenzhen Planck Innovation Technologies Co. Ltd., Shenzhen 518173, China

[a)]Author to whom correspondence should be addressed: xwsun@sustech.edu.cn

Device Fabrication and Characterization

Materials

PEDOT:PSS is purchased from Luminescence Technology Corp. Poly[(9,9-dioctylfluorenyl-2,7-diyl)-co-(4,4'-(N(p-butylphenyl))diphenylamine)] (TFB, molecular weight 136000 (PS Standards)) are from American Dye Source. CdSe/ZnS Quantum dots are from Suzhou Xingshuo Nanotech Company, Ltd.. The ZnO nanocrystals are synthesized in the lab. The sheet resistance of pre-patterned ITO is 20 Ω/□.

Device Fabrication Process

In the work, QLEDs are with normal structure indium tin oxide (ITO)/PEDOT:PSS (~30 nm)/TFB (~30 nm)/QDs (~40 nm)/ZnO (~40 nm)/Ag (100 nm). The patterned ITO is ultrasonic cleaned with acetone, deionized water and isopropanol under 15 min followed by oxygen plasmas cleaning. Detailed process parameters are listed in Table S1. After fabrication, the devices are well packaged with UV resin (LOCTITE 3335) and encapsulation glass in the glove box immediately.

Table S1: Processes parameters of QLEDs fabrication in the work.

Layer	Rotational Speed (rpm)	Temperature (°C)	Annealing Time (min)	Concentration (mg/ml)	Note
PEDOT:PSS	3000	130	15	-	Air
TFB	3000	120	10	8	Glove box
QD	3000	100	5	15	Glove box
ZnO NC	3000	100	10	20	Glove box
Ag	-	-	-	Thickness 100 nm	Chamber 0.5 - 1 nm/s

Characterization

The J-V-L and EQE characteristics of the devices are measured by an integrating-sphere combined with KEITHLEY 2400 source meter and OCEAN OPTICS USB200+ spectrometer. Capacitance-voltage characteristics are tested using an impedance analyzer (HP4284A) at f = 1kHz, V_{ac} = 100 mV. All characterizations are performed at room temperature. The aging test is performed by the OLED/QLED Lifetime Test System, which has the fixture embedded with and photodiode. Time-resolved electroluminescence (TREL) is based on the microscope with an integrated light path and TCSPC as a detector. The trigger signal is from the signal generator (f = 50 MHz).

Supplementary Results

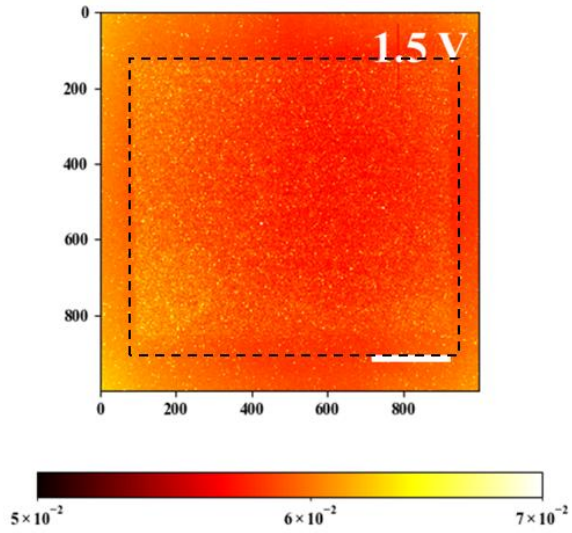

Fig. S1: Luminance distribution of device under 1.5 V bias. Weak but uniform emission can be deserved indicating the turn-on and recombination of electrons and holes. (Scale bar 500 μm, active area is marked with black dashed box).

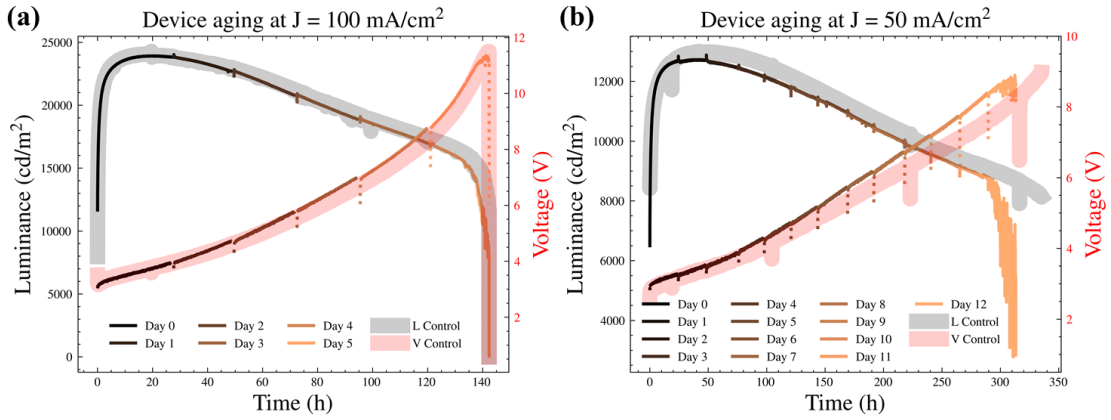

Fig. S2: Luminance and voltage degradation behaviour with aging time. All of devices are aging at constant current mode with (a) J = 100 mA/cm^2, (b) J = 50 mA/cm^2. The data with thick and semitransparent lines is the control device test without discontinuity.

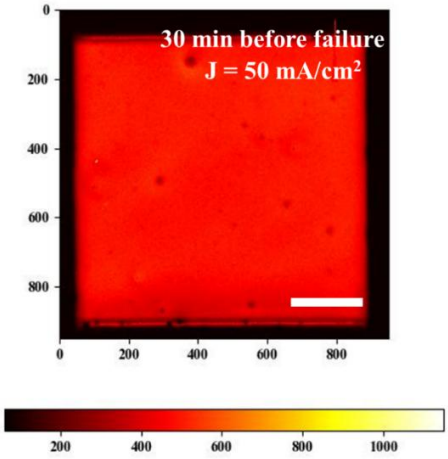

Fig. S3: Luminance uniformity check by imaging photometer. The uniform emission before device failure shows the device degradation is global and uniform in the whole test (J = 50 mA/cm^2, Scale bar 500 μm).

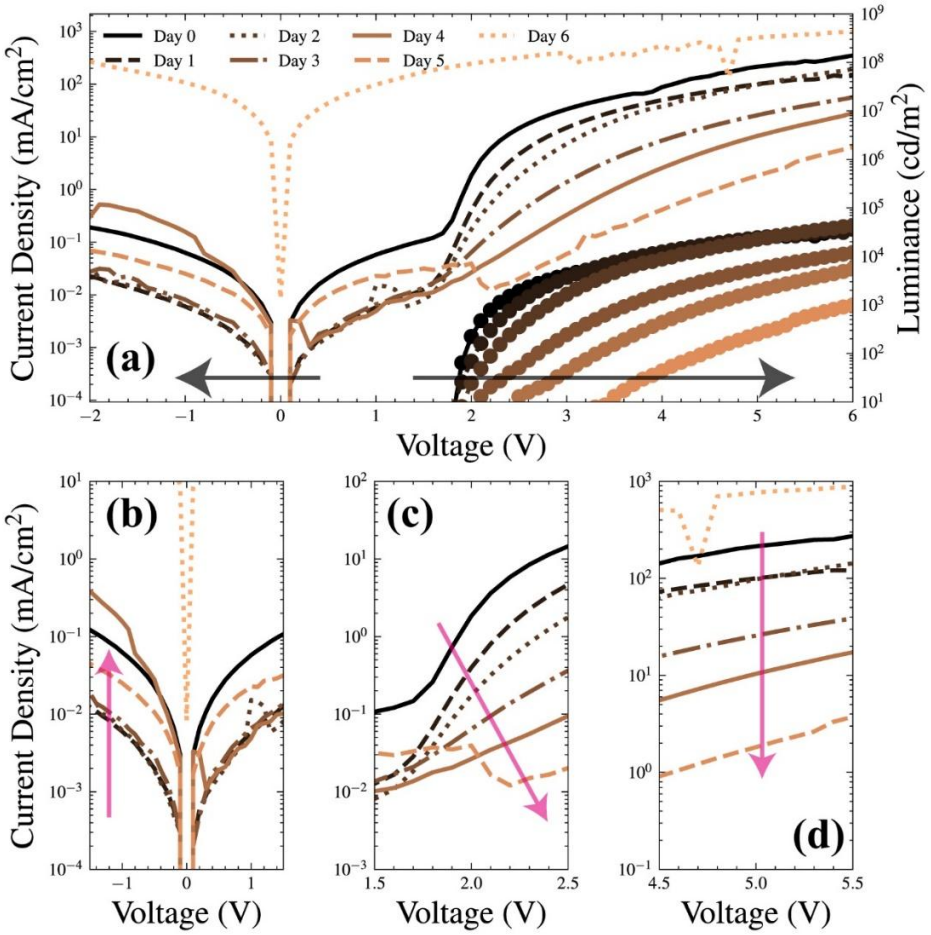

Fig. S4: J-V-L degradation of device aging at J = 100 mA/cm2. (a) is the survey, (b)-(d) are the region for leakage, recombination, and large forward current. During the aging, the leakage is increasing, and the recombination and bulk resistance is also increasing.

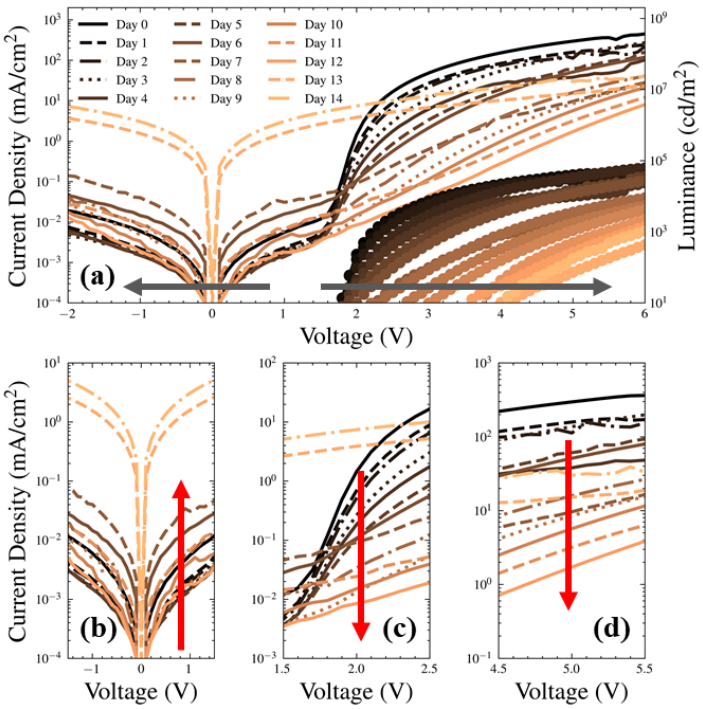

Fig. S5: J-V-L degradation of device aging at J = 50 mA/cm^2. (a) is the survey, (b)-(d) are the region for leakage, recombination, and large forward current. Similar behaviour is observed compared with J = 100 mA/cm^2 (Figure S4).

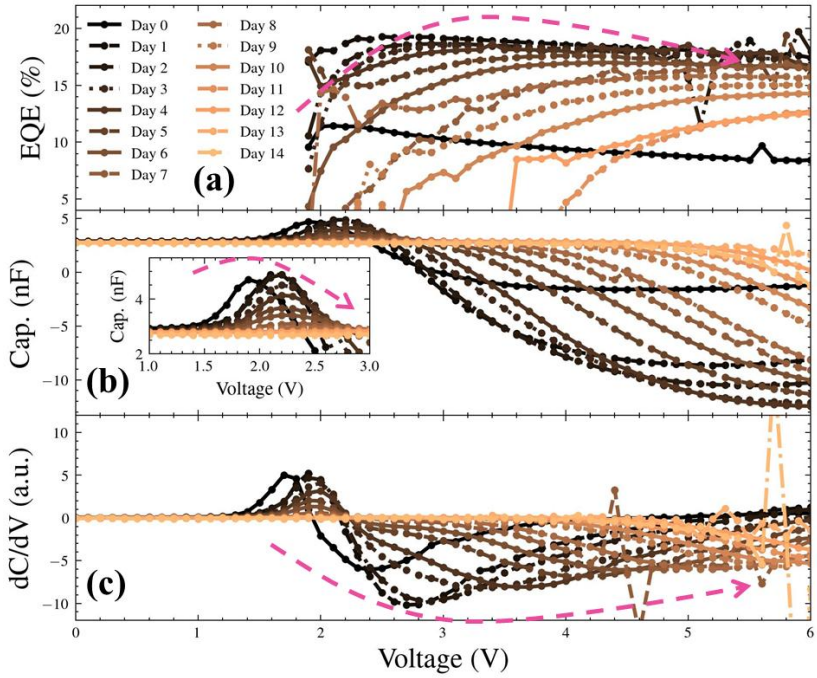

Fig. S6: Aging time-dependent characteristics of QLED. The device is stressed with constant J = 100 mA/cm^2. (a) EQE, (b) C-V (inset is the zoom of charge accumulation region) and (c) dC/dV. Similar behaviour is observed compared with J = 50 mA/cm^2 (Figure 4).

Table S2: Comparison of C-V and dC/dV-V measurements for QLEDs.

Item	**dC/dV-V**	**C-V**
V_T (Turn-on voltage)*	Yes*	Yes*
V_j (Charge injection voltage)**	Yes	N/A
V_{EQEmax}	Yes, voltage at minimum of dC/dV	N/A
C_g (Geometric capacitance)	N/A	Yes, C_0 (C under 0 V bias)
Charge accumulation	N/A	Yes, C_{peak}

* Turn-on voltage value (V_T) reflected by dC/dV is smaller than by C-V.
** V_j means the charge injection voltage for the charge unbalanced device.